Vibrational Dynamics of Carbon Monoxide at the Active Site of Myoglobin: Picosecond Infrared Free-Electron Laser Pump−Probe Experiments

Jeffrey R. Hill,[†] A. Tokmakoff,[‡] Kristen A. Peterson,[§] B. Sauter,[‡] D. Zimdars,[‡] Dana D. Dlott,[*,†] and M. D. Fayer[*,‡]

School of Chemical Sciences, University of Illinois at Urbana−Champaign, 505 S. Mathews Avenue, Urbana, Illinois 61801, Department of Chemistry, Stanford University, Stanford, California 94305, and Hansen Experimental Physics Laboratory, Stanford University, Stanford, California 94305

Received: April 27, 1994; In Final Form: July 20, 1994[⊗]

The vibrational lifetimes of CO stretching modes of CO bound to different conformational substates of myoglobin, and CO bound to a water-soluble bare Fe:porphyrin, Fe tetraphenylporphyrin sulfate, were measured by picosecond infrared (IR) pump−probe experiments using the Stanford Free Electron Laser. At room temperature, two substates of carboxymyoglobin (Mb-CO), denoted A_0 and A_1, yielded lifetimes of 26.6 ± 1 and 18.2 ± 1 ps in a poly(vinyl alcohol) matrix. In glycerol:water solution, the A_1-state lifetime of Mb-CO was 17.4 ± 1 ps. These lifetimes do not depend much on temperature in the 20−300 K range. The lifetime of the bare Fe:porphyrin was 17 ± 3 ps. Results obtained on these and other heme−CO systems are used to show that vibrational relaxation is slower with CO whose frequency is close to the ~1970 cm^{-1} value characteristic of proteins and model compounds with CO nearly perpendicular to the heme plane, and faster with CO with lower frequencies characteristic of hindered CO. It is also shown that different conformational substates of the same protein can have different vibrational relaxation rates at the active site and that different substituents on the perimeter of the porphyrin may significantly affect the vibrational relaxation.

I. Introduction

Carboxymyoglobin (Mb-CO) consists of an ≈18 kDa protein, a chromophoric prosthetic group, protoheme (Ph, also denoted protoporphyrin-IX), and a CO ligand bound to Fe at the active site of the protein (see Figure 1a,b).[1] Spectroscopic studies of the CO stretching vibration[2] have proven to be an important window to protein dynamics at the active site.[3−7] Bound CO is termed the A state.[3,4] Photolyzed CO in the protein pocket is termed the B state.[3−4] Both A and B states have been observed via relatively intense mid-IR absorptions near 5.1 and 4.7 μm, respectively.[3]

Until very recently, mid-IR studies of Mb-CO could be divided into two types: (1) analyses of the absorption spectrum of CO,[2−5] and (2) time-resolved studies of photoinduced CO dissociation and rebinding, probed using weak mid-IR light.[6−8] A new method now exists to investigate vibrational dynamics of CO bound at the active site of Mb or other heme systems,[9−11] using an IR pump−probe technique which measures the loss of vibrational energy from the CO stretching vibration following its excitation by an intense picosecond mid-IR pulse.[12,13] Unlike the older methods, which needed only weak probe light in the mid-IR, the pump−probe technique requires an apparatus which can generate intense, ultrashort tunable mid-IR pump pulses. In this work, experiments are performed on CO bound to spectroscopically distinct sites of Mb and on CO bound to a water-soluble model heme compound with no protein, Fe tetraphenyl porphyrin sulfate (Fe:TPPS; see Figure 1c) using pulses generated by the Stanford Free Electron Laser (FEL).[14] This technique provides a direct probe of vibrational energy transfer at the active site of the protein, which occurs on a time scale readily accessible to molecular dynamics calculations (typically 0−0.1 ns).

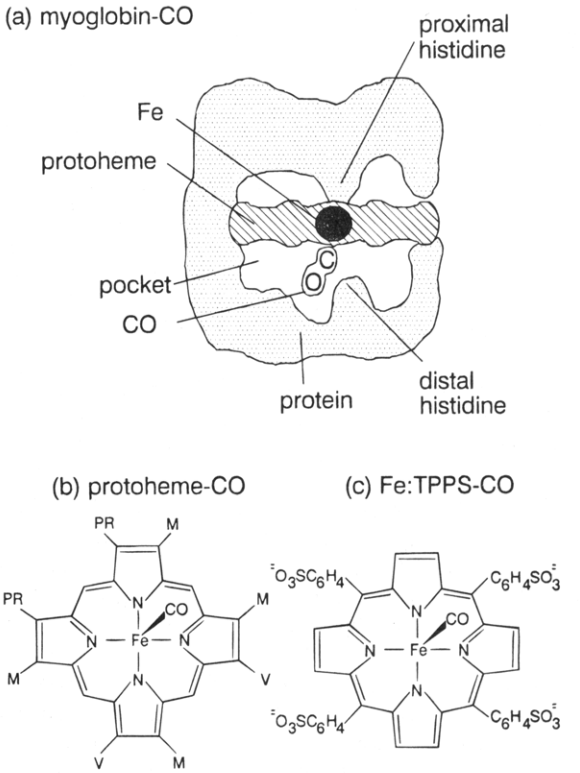

Figure 1. (a) Schematic diagram of myoglobin-CO (Mb-CO). (b) Structure of protoheme (Ph), the prosthetic group in Mb. Key: M = CH_3, V = CH = CH_2, PR = $CH_2CH_2CO_2H$. (c) Structure of Fe tetraphenylporphyrin sulfate (Fe:TPPS).

Some relevant results from prior studies of Mb-CO are as follows:

[†] University of Illinois at Urbana−Champaign.
[‡] Department of Chemistry, Stanford University.
[§] Hansen Experimental Physics Laboratory, Stanford University. Permanent address: Department of Chemistry and Biochemistry, New Mexico State University, Las Cruces, NM 88033.
[⊗] Abstract published in *Advance ACS Abstracts,* October 1, 1994.

0022-3654/94/2098-11213$04.50/0

(a) The mid-IR absorption of Mb-bound CO consists of at least four distinct bands, denoted A_0–A_3, in order of decreasing frequency.[4] These bands evidence inhomogeneous broadening and can be fit by Voigt line shapes,[4] i.e., the convolution of a Gaussian and a Lorentzian function.

(b) The distinct mid-IR absorption bands of bound CO apparently occur due to the coexistence of different protein conformational substates.[4] The frequency shifts of bound CO in different protein conformations have been attributed by various authors to steric-induced bending of the Fe–CO bond (e.g. ref 15) or electrostatic effects arising from interactions between the CO dipole and differing charge distributions in the protein pocket (e.g., ref 16). A more recent detailed study and discussion attributes frequency shifts to differing distal polar interactions,[17] arguing that the protein does not generate large enough steric effects to tilt the CO, and it suggests the following picture: in A_0, protonation of the distal histidine imidazole causes it to swing out of the heme pocket, leaving an unhindered CO almost normal to the heme plane, a conformation similar to that found in bare porphyrins such as Ph-CO;[4,5,17] in A_{1-3}, electrostatic interactions between unprotonated distal histidine and the π^* orbital of CO induce bending and frequency lowering.

(c) The spectral peak centers, relative intensities, line widths, and oscillator strengths of these A states are detectably influenced by environment, specifically solvent, pH, the conformation of the protein matrix, and temperature.[4] In Mb at pH = 7.0 in a solid matrix of poly(vinyl alcohol) (PVA), the A_1 and A_0 states have about equal intensities.[4]

(d) The properties listed above have a relatively weak dependence on temperature in the 50–300 K range. In glycerol:water, there is almost no temperature dependence below 180 K.[4] Some properties such as the mid-IR line width show an abrupt change near 180 K, whereas other properties such as the peak frequency shift show a gradual change in the 300–180 K region.[4] These dependences were interpreted to arise from a solvent glass-transition at $T_g \approx 180$ K, which in turn induces a transition in the protein matrix termed a "slaved glass transition".[4,5] In PVA, a solid throughout the 50–300 K range, almost no temperature dependence is observed in this range.[4]

(e) Interconversion among A states is possible,[2] even in the absence of light which can photolyze Mb-CO. The interconversion rate in glycerol:water at 300 K is estimated[5] at $k \approx 10^7$ s^{-1}. The rate decreases with decreasing T, and interconversion is not observed below 180 K.[4] In PVA, a solid at room temperature, interconversion is not seen at 300 K or below.[4]

Hochstrasser and co-workers recently gave a quite brief report of picosecond pump–probe relaxation times for the A_1 state of Mb, hemoglobin-CO (Hb-CO), and Ph-CO in D_2O solution at ambient temperature to be 18, 18, and 31 ps, respectively.[9] In the present work, we report pump–probe data on Mb-CO in glycerol:water and in PVA, where more than one A state can be studied, and on Fe:TPPS-CO. In addition, we report detailed temperature-dependent data on Mb-CO. These results are used to investigate the mechanisms of molecular vibrational energy transfer at the active site of proteins, and the relationships between molecular structures and the rates of energy transfer.

II. Experimental Section

Preparation of the Mb-CO sample follows the general procedure outlined previously.[2] To maximize the ratio of bound CO absorbance to background, a high protein concentration and a small optical path length were used. The glycerol:water samples used horse heart Mb (Sigma) at ~30 mM concentration in glycerol:water (60:40), buffered to pH = 7.0 with sodium phosphate. The use of 60:40 glycerol:water instead of the more typical 75:25 glycerol:water[3] allowed us to approximately double the protein concentration to roughly 30 mM. The samples were held in a 0.1 mm path cell with 1 mm thick sapphire windows. The optical cell could be mounted in a closed-cycle He refrigerator with CaF_2 optical windows. The PVA samples[3] were prepared as above except instead of glycerol:water, a solution of 10 wt % PVA dissolved in 1 mM phosphate buffer at pH = 7.0 was used. The Mb-CO in PVA solution was spread onto a sapphire window and allowed to dry and harden under 1 atm of CO. Assuming that most of the water evaporated during drying, the concentration of Mb-CO in the dried PVA film was estimated at 30 mM, and the concentration of phosphate buffer after drying should be similar to that used above. The thickness of the film varied considerably over the area of the sapphire window, and the PVA film scattered more IR light than the glycerol:water samples.

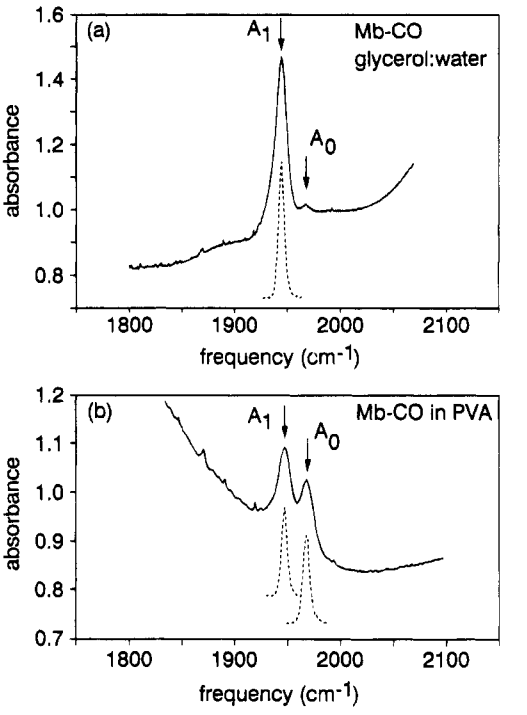

Figure 2. Mid-IR spectrum of Mb-CO in glycerol:water and in poly(vinyl alcohol) (PVA) in the vicinity of the bound CO A-state stretching absorptions. The dashed curves are the spectra of free-electron laser pulses used in pump-probe experiments.

Mid-IR spectra of Mb-CO A states in glycerol:water and in PVA are shown in Figure 2. Because the IR beam is several millimeters in diameter, the PVA spectrum represents an average over regions of considerably varying thickness. The ~100 μm diameter spots chosen for pump–probe experiments probably had optical densities comparable to the glycerol:water samples. The locations of the absorption maxima are within apparatus resolution (0.2 cm^{-1}) identical to those reported previously[4] despite minor differences in sample preparation (e.g., horse-heart Mb at pH = 7.0 rather than sperm whale Mb at pH = 6.8). Fe:TPPS is an Fe:porphyrin with excellent water solubility. Fe:TPPS was synthesized from tetraphenylporphyrin by addition of H_2SO_4, followed by metallation. The Fe:TPPS-CO sample consisted of 30 mM Fe:TPPS in glycerol:water (75:25) at pH = 10.0. The pH was adjusted by adding NaOH. The IR spectrum of Fe:TPPS is shown in Figure 3. The substantial background in the spectra in Figures 2 and 3 is caused by window reflection and solvent and protein absorption.

The Stanford superconducting linear accelerator pumped picosecond free-electron laser (FEL)[14] emits a 2 ms duration

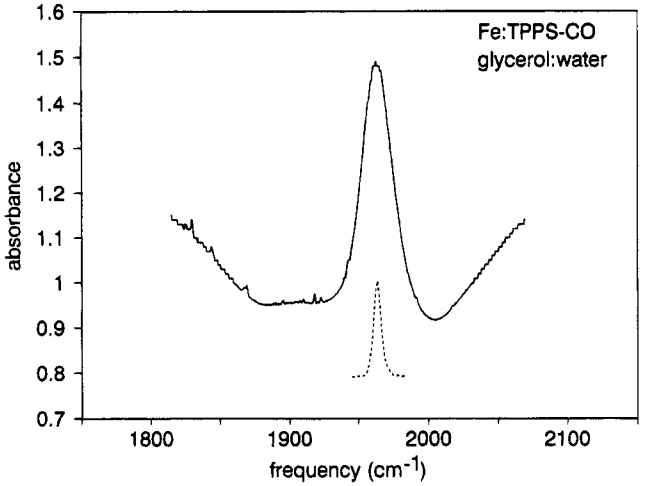

Figure 3. Mid-IR spectrum of Fe:TPPS-CO in glycerol:water. The dashed curve is the spectrum of free-electron laser pulses used in pump-probe experiments.

macropulse at a 10 Hz repetition rate. Each macropulse consists of $\sim 2.3 \times 10^4$ micropulses of $\sim 0.5\ \mu$J energy, at a micropulse repetition rate of 11.7 MHz. The micropulses were measured to be Gaussian ~ 2 ps transform limited pulses (spectral bandwidth ~ 7.3 cm^{-1} fwhm) by autocorrelation in a $AgGaSe_2$ crystal.[18,19] The FEL output pulse spectra used in these experiments, measured over a ~ 60 s interval using a 1 m scanning spectrometer and a mid-IR sensitive optical detector, are also shown as dashed curves in the absorption spectra of Figures 2 and 3. The FEL center wavelength was stable to within an accuracy of 0.2 cm^{-1} during these experiments. At the sample, the pump pulse was 150 nJ, and the probe pulse was 15 nJ. The micropulse repetition rate was reduced to 50 kHz by a germanium acousto-optic single pulse selector.[19,20] The effective experimental repetition rate is 1000 pulses/s. A dual beam geometry was used with two HgCdTe detectors, two gated integrators, and computer with 16-bit analog-to-digital converter to measure intensities of probe and reference pulses. The probe intensity was divided by the reference intensity to normalize intensity fluctuations. The pump beam was chopped with a second pulse selector, so pump pulses arrived at the sample at 25 kHz and probe pulses at 50 kHz. On adjacent chopped and unchopped pulses, normalized probe signals were divided and the log taken, to yield the shot-normalized pump-induced absorbance change. A stepper-motor-driven retroreflector varied the delay between pump and probe pulses. An autocorrelator and mid-IR optical spectrometer continuously monitored the FEL pulse duration and pulse spectrum.

III. Results

A. Spectroscopy of A-States. The mid-IR spectroscopy of Fe:TPPS-CO in glycerol:water had not been studied previously. Figure 3 shows a single Fe:TPPS-CO absorption band, which is almost frequency-coincident with the A_0 state of Mb-CO. The Fe:TPPS-CO absorption band can be accurately fit to a Gaussian line shape centered at 1963.7 cm^{-1} with a fwhm of 27 cm^{-1}, more than double the fwhm of the A_1 state of Mb-CO.

Gaussian line shapes are frequently indicative of inhomogeneous broadening of a spectral line. In a liquid such as the glycerol:water mixture used as the solvent for Fe:TPPS-CO, on some time scale any solute molecule will sample all possible solvent configurations. For the line to appear inhomogeneously broadened, it is only necessary that the homogeneous line width be small compared to the spread of transition energies associated with different solvent environments. The Gaussian line shape

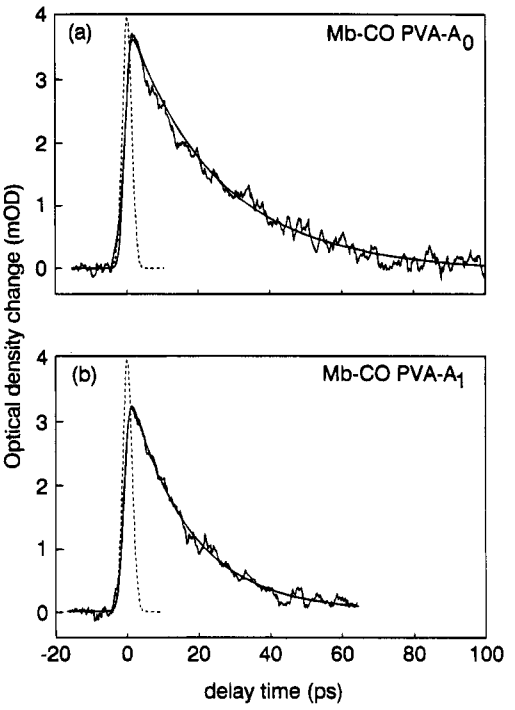

Figure 4. (a) Pump−probe decays (absorption transients), which measure vibrational relaxation (VR) of the A_0 and A_1 states of Mb-CO in poly(vinyl alcohol) (PVA) at ambient temperature, obtained using 2 ps duration mid-IR pulses from the Stanford Free Electron Laser (FEL). The displayed data points at 0.2 ps intervals were processed with a 7-point smoothing algorithm. The dashed curves are optical autocorrelations of the mid-IR pump and probe pulses, which give the apparatus time response. The smooth curves are the computed convolution of a Gaussian apparatus response with an exponential decay. The different exponential decay constants of 26.6 and 18.2 ps demonstrate that different protein conformations can affect energy transfer rates at the active site.

for Fe:TPPS-CO is consistent with inhomogeneous broadening that can arise from the wide variety of local solvent structures which exist in hydrogen-bonding solvents. The substantially narrower absorption line width of Mb-CO relative to Fe:TPPS-CO, and the appearance of an Mb-CO absorption line shape which cannot be fit by a simple Gaussian,[4] both of which result from effects of the protein matrix, suggest the protein yields a more limited number of local environments, or a set of local environments which induces a smaller spread of transition energies compared to the solvent environment of a bare Fe-heme.

B. Lifetimes of CO Stretches in Mb-CO and Fe:TPPS-CO. The FEL was used to measure the lifetimes of bound CO stretching vibrations in Mb and Fe:TPPS, as shown in Figures 4 and 5. When the FEL was tuned off the absorption peaks, no absorption transients were observed, because the off-resonant background is caused by a high concentration of absorbers which cannot be optically saturated due to their smaller absorption cross-sections. The bound CO absorptions can be appreciably saturated due to their far larger cross sections, e.g., in the Mb-CO A_1 state in glycerol:water, $\sigma \approx 8 \times 10^{-17}$ cm^2. With the FEL tuned to either the A_0 or A_1 state absorption maxima of Mb-CO PVA samples, the pump−probe signals (absorption transients) shown in Figure 4 were measured. With PVA, the samples were translated through the FEL beam to find spots which gave minimum light scattering and optimal signal to noise. At these spots, the peak absorbance changes were $\Delta A = 3-4$ mOD. The two A-states gave noticeably different time dependences, as shown in Figure 4. The decays were determined by least-squares fitting to be exponential over at least

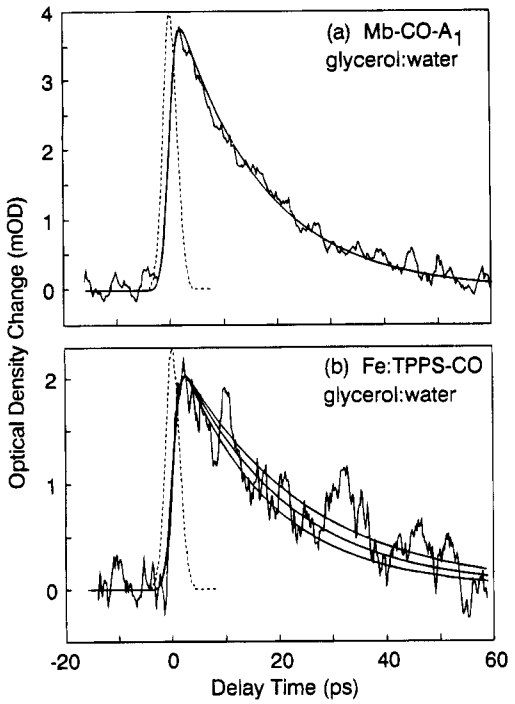

Figure 5. (a) Pump−probe data which measures the ambient temperature decay of vibrational excitation of the A_1 state of Mb-CO in glycerol:water. (b) Ambient temperature decay from Fe:TPPS-CO in glycerol:water. The dashed curves are optical autocorrelations of mid-IR pump and probe pulses. The solid curves are computed convolutions of a Gaussian apparatus response with an exponential decay. The exponential decay constant for Mb-CO in glycerol:water was $\tau = 17.4 \pm 1$ ps. For Fe:TPPS-CO the decay constant was $\tau = 17 \pm 3$ ps. In part b, the smooth curves which bracket the data were computed using decay constants $\tau = 14$, 17, and 20 ps.

five factors of e. The decay constants in PVA were $\tau = 18.2 \pm 1$ ps for the A_1 state and $\tau = 26.6 \pm 1$ ps for the A_0 state. Here the error bounds denote 1 standard deviation from the best-fit exponential.

For Mb-CO in glycerol:water, the absorption transient shown in Figure 5a was observed when the FEL was tuned to the A_1-state absorption maximum. The decay was also exponential over at least five factors of e, and the time constant was $\tau = 17.4 \pm 1$ ps. The Fe:TPPS-CO data in Figure 5b was noisier than Mb-CO data, and it gave a time constant of $\tau = 17 \pm 3$ ps. For Fe:TPPS-CO, the error bars were determined by bracketing the data with different computed fitted curves, as shown in Figure 5b.

In all these experiments, the time-dependent recovery of mid-IR absorption is attributed, as in previous works,[12,13] to vibrational energy relaxation of the excited CO stretching mode. Ambient temperature decay constants measured in this work and by Hochstrasser et al.[9] are summarized in Table 1.

C. Temperature Dependence of Mb-CO Vibrational Lifetime. Pump−probe data were obtained at different temperatures in the 20−300 K region. The measured temperature-dependent decay times are plotted in Figure 6. The broken horizontal lines are visual guides. The estimated error bars on the data (1 standard deviation) are smaller than the points used to represent the data. Within experimental error, no dependence on temperature was observed for the PVA samples. The A_1 state of Mb-CO in glycerol:water did evidence some temperature dependence in cooling the sample from 300 to ~200 K. The decay time constant gradually increased from 17.4 to ~21 ps in this range, and this increase, although small, is clearly discernible with our apparatus. Below ~200 K, the decay time constant is independent of temperature.

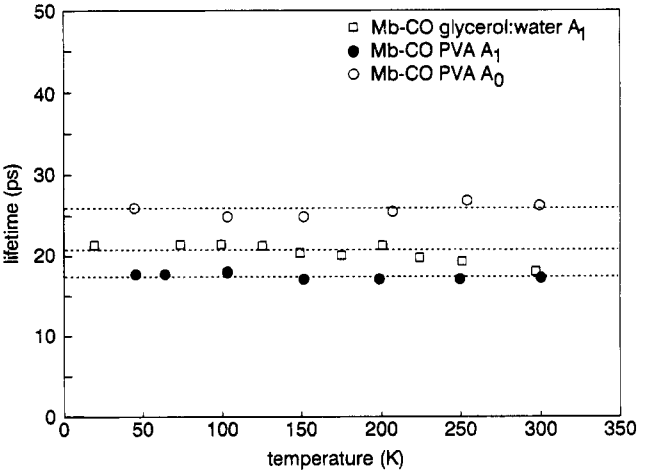

Figure 6. Temperature dependence of CO vibrational relaxation (VR) rates in myoglobin in glycerol:water or PVA. The dashed lines are visual guides. The A_1 state of Mb-CO in glycerol shows a small but detectable decrease in VR rate between 300 and 200 K. The VR rates in PVA do not change detectably with temperature.

IV. Discussion

A. Pump−Probe Experiments and Optical Line Shapes. The pump−probe experiment measures the time-dependent recovery of mid-IR absorption following a bleaching induced by the pump pulse. The recoveries in Mb-CO and Fe:TPPS-CO appear to be single exponentials. Our interpretation of this effect follows that of Heilweil et al.[12] and other recent work[13] on the vibrational lifetimes of CO bound to metals in liquid solution. The CO vibration can be treated as a saturable two-level system because of the significant frequency mismatch between the $v = 0 \rightarrow v = 1$ and the $v = 1 \rightarrow v = 2$ transitions, which for heme-CO is about 25 cm^{-1}.[10] Care was taken to make sure that with the powers and bandwidths used in the experiments reported here, only the $v = 0 \rightarrow v = 1$ transition was excited. Absorption recovery mechanisms involving significant contributions from spectral diffusion to other A states or within the inhomogeneously broadened A_1 transition seem highly unlikely because interconversion in PVA does not occur,[4] and in glycerol:water, the decays at ambient temperature are hardly different from decays below 180 K, where interconversion among various A states ceases and other spectral

TABLE 1: Vibrational Lifetimes of CO Bound to Various Hemes

molecule	solvent	freq (cm^{-1})	lifetime T_1 (ps)
protoporphyrin-IX Mb-A_1	glycerol:water 60:40, pH = 7.0	1943	17.4 ± 1
protoporphyrin-IX Mb-A_1	D_2O	1944[a]	18[a]
protoporphyrin-IX Mb-A_1	poly(vinyl alcohol) (PVA), pH = 7.0	1946	18.2 ± 1
protoporphyrin-IX Mb-A_0	poly(vinyl alcohol) (PVA), pH = 7.0	1967	26.6 ± 1
protoporphyrin-IX Hb	D_2O	1951[a]	18[a]
protoporphyrin-IX	D_2O	1977[b]	31[a]
Fe tetraphenylporphyrin sulfate	glycerol:water 60:40, pH = 10.0	1964	17 ± 3

[a] Reference 10. [b] Reference 2.

diffusion mechanisms should slow. We thus identify the exponential time constant, τ, as characterizing the time-dependent flow of vibrational energy out of the ensemble of vibrationally excited CO molecules. (In the discussion below, VR is used to denote vibrational energy relaxation. Some authors use VR to denote vibrational phase relaxation.)

The exponential time constants measured here, on the order of $\tau = 15-30$ ps, correspond to frequency-domain Lorentzian line widths[21] of $\Delta\nu = 0.1-0.3$ cm^{-1}. Therefore, the contribution of VR to the broad vibrational line shapes seen in Figures 2 and 3 is negligible. The substantial Lorentzian component of the Mb-CO vibrational absorption line[4] cannot be explained by VR. It can be attributed to either pure dephasing processes[21] or a temperature-dependent Lorentzian inhomogeneous broadening mechanism.[22]

B. Mechanisms of Vibrational Relaxation (VR). Previous work shows that VR does not involve electronic degrees of freedom of the metal atom, but rather occurs via mechanical energy transfer between excited CO and other vibrations in the system.[12,13] Our interpretation of the mechanisms of VR in heme−CO systems is based on two significant facts: (1) the frequency of the excited vibration, $\nu \sim 1950$ cm^{-1}, is far above the threshold energy for efficient intramolecular vibrational redistribution (IVR) in gas-phase porphyrin, which is known[23] to be about 700 cm^{-1}, and (2) the dependence of the VR rate of Mb-CO on temperature is small in glycerol:water and negligible in PVA.

In an isolated molecule, the density of internal vibration states increases with increasing energy. Lower energy vibrational excitations cannot undergo IVR due to the impossibility of finding relaxation pathways which conserve energy. The IVR threshold denotes an approximate level of excess vibrational energy where the density of internal states becomes large enough to permit efficient irreversible decay of energy from an initially prepared state. Ordinarily IVR is viewed as the relaxation of an excited anharmonic local mode oscillator coupled to a set of doorway states which open up the remainder of the molecule for the vibrational energy.[24,25] Condensed matter molecular systems are quite different due to the presence of a bath. In condensed matter, VR can occur even in the lowest energy vibrations due to anharmonic coupling between molecular vibrations and the bath.[26]

In the present case of heme-CO, the pump pulse excites an ensemble of excitations which are essentially localized on CO. A large density of states must be present at the ~1950 cm^{-1} energy of the CO excitation because the observed decay is fast, irreversible, and exponential in time. The VR process may involve several steps, such as sequential loss of CO excitation to the doorway vibrations followed by loss of energy from the doorway vibrations into the bath.

As seen in Figure 1, in Mb (and in Hb) CO is covalently bound to Fe, which has five other ligands, four equatorial ligands donated by the tetradentate porphyrin, and one axial ligand being the proximal histidine residue of the protein. Thus, likely candidates for doorway modes are vibrational motions which involve larger amplitude oscillations of Fe−C and Fe−N bonds. Resonance Raman spectroscopy[17,27,28] reveals the presence of many Ph vibrations in the 100−1700 cm^{-1} range, including the Fe−CO stretch at ~510 cm^{-1}, the Fe−C−O bend at ~575 cm^{-1}, and the Fe−His stretch at ~210 cm^{-1}. The bath states can be identified as being nondoorway vibrations of the porphyrin, solvent vibrations, the lower frequency continuum of instantaneous normal modes (phonons) of the solvent,[13,29] protein vibrations, lower frequency collective protein modes,[30−31] etc.

Lowering the temperature reduces the rates of any VR processes which are thermally activated by excited vibrations of energy $\leq kT$. The rate of vibrational energy loss from CO will be activated by thermal excitations of the significant doorway modes. The lack of much temperature dependence in Figure 6 therefore indicates that no doorway modes are becoming excited in the 20−300 K range. We conclude the doorway modes involved in CO vibrational relaxation must be higher in energy than ~400 cm^{-1}, or else their effects would have been seen in Figure 6. This observations rules out the Fe−His stretching mode, solvent phonons, or collective protein modes as being important doorway states.

C. Vibrational Relaxation and Protein Function. Our observation that different A states in Mb-CO can have different VR decay constants is highly significant. *It shows unambiguously that different conformational substates of the same protein can have different rates of vibrational energy transfer at the active site.* Another way of putting this conclusion is to say that different conformations of the same protein can influence the rates of energy transfer at the active site.

It is interesting to compare our vibrational energy transfer measurements to what is known about protein function. Experiments which monitor the rebinding of CO to Mb in glycerol: water following flash photolysis below 180 K (i.e., in the regime where interconversion between A states does not occur) show that different A states rebind CO with different kinetics[4] and that the rebinding of CO to individual A-states is nonexponential in time.[4] Several models have been advanced to explain this nonexponential rebinding. In a bit of oversimplification appropriate here, these models may be classed as either inhomogeneous or homogeneous. In an inhomogeneous model proposed by Frauenfelder et al., functionally different proteins coexist (e.g., ref 4 and references therein). Mb exists below 180 K in a static distribution of hierarchical conformational substates.[4,32] The highest tier of substates, denoted CS^0, is composed of the A states, i.e., states characterized by discernibly different heme−CO stretching bands. A lower tier CS^1, consisting of different protein conformations, at least some of which rebind CO at different rates, has been postulated to explain the nonexponential rebinding. In homogeneous models, all proteins are assumed to be functionally identical. Nonexponential rebinding is then explained by various models (e.g., refs 33−35, among others), including a time-dependent relaxation process subsequent to photolysis[33] or the existence of many independent pathways for ligand rebinding within a single protein.[34−35] When we perform a pump−probe experiment on an A state, we observe an exponential decay, proving that all the proteins excited by the laser pulse (as shown in Figures 2 and 3, our laser pulse spectrum is somewhat narrower than the A-state spectrum) have indistinguishable VR kinetics. In terms of the two classes of models described above, this observation shows that either the ensemble of proteins which compose a particular A-state are homogeneous, or if inhomogeneous, the different CS^1 substates of a particular substate of CS^0 do not have significantly different VR rates.

D. Vibrational Relaxation and Molecular Structure. Using the data in Table 1, we have plotted VR decay rate constants versus vibrational frequency, as shown in Figure 7. In Figure 7, all the compounds which contain Ph lie on a line also shown in the figure. The correlation coefficient of the least-squares fitted line is $R = 0.982$. The TPPS point, which is from the only compound with a differently structured porphyrin, lies well off this line. Figure 7 immediately suggests two conclusions: (1) the VR rate constant apparently shows no significant dependence on the nature or viscosity of the solvent;

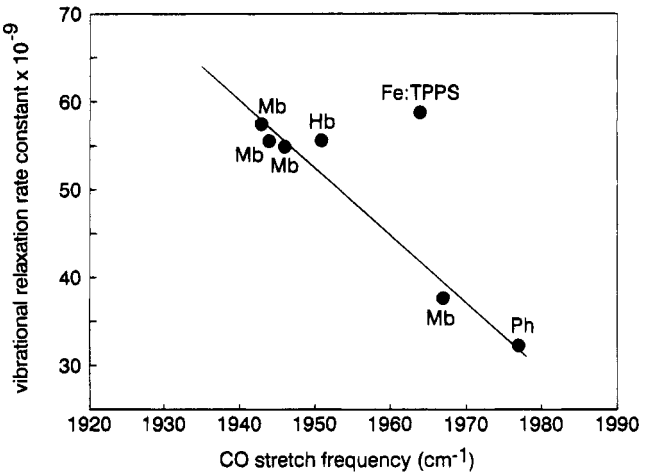

Figure 7. Plot of CO vibrational relaxation rate constant versus CO stretch frequency for the compounds listed in Table 1. For the compounds myoglobin (Mb) and hemoglobin (Hb), which contain protoheme (Ph), and for bare Ph itself, linear least-squares fitting was used to compute the best-fit line. The Fe:TPPS point, obtained from a meso-substituted porphyrin whose substituents differ from Ph, lies well off this line.

and (2) the VR rate constant for Fe:TPPS is significantly different than that of protoheme-containing compounds with similar CO stretching frequencies, suggesting that VR depends significantly on the structure of the porphyrin moiety.

With the available data in Figure 7, we cannot distinguish with certainty between two interesting possibilities: either (1) the VR rate constant increases linearly with decreasing CO stretch frequency in systems containing protoheme; or (2) the VR lifetime T_1 in systems containing protoheme can take on either of two possible values, $T_1 \sim 30$ ps for unhindered CO almost normal to the heme plane, and $T_1 \sim 18$ ps for hindered CO. These possibilities could be distinguished by further investigations of new heme proteins created by site-directed mutagenesis,[36] in order to determine whether there exists only one type of hindered environment with $T_1 \sim 18$ ps, or a range of hindered environments with intermediate values of T_1.

We now consider some aspects of the influence of protein and heme structure on VR. In the A_1 state of Mb, the CO VR time constant is reduced by a factor of ~50% relative to the A_0 time constant or the Ph-CO time constant. There are two possible explanations for the lifetime reduction in the A_1 state: either the A_1-state conformation permits an additional energy-transfer pathway from excited CO to the protein, especially the proximal histidine residue, or the increased hindrance[17] of CO in the A_1 state enhances the coupling between excited CO and the doorway modes. We favor the latter interpretation because ordinarily noncovalent interactions between CO and the protein are weaker than the covalently bonded interaction between CO and Fe.

The two bare porphyrin compounds, protoheme and Fe:TPPS, have CO stretching frequencies which both lie in the higher frequency range of the compounds examined here. The different VR rates for these two compounds suggest the possibility that porphyrin structure can substantially influence VR. In comparing these two compounds, one should keep in mind that Fe:TPPS data were obtained in glycerol:water solvent, whereas Ph data were obtained in D_2O solvent which results in a different local solvent configuration and different proximal ligation. It does seem likely, however, that the effects of solvent are less than the effects of heme structure. For example, two protoheme-CO compounds with higher frequency CO stretching vibrations but very different solvent environments, Ph-CO in D_2O and the A_0 state of Ph-CO in Mb, are found to have similar VR rates.

Effects of porphyrin structure on VR rates may be explained in two possible ways: either Fe:TPPS increases the rate of energy transfer from excited CO to the doorway modes, or Fe:TPPS increases the rate of energy flow from the doorway modes into the bath. We favor the latter explanation. Both compounds have identical structures in the vicinity of the Fe-CO group, but differ at the molecular perimeter. Protoheme is a pyrrolic-substituted porphyrin, whereas Fe:TPPS is a meso-substituted porphyrin. The combined masses of the four sulfoxyphenyl groups on TPPS (MW = 624) is ~2.4 times greater than the combined masses of the protoheme substituent groups (MW = 260). The effects of these heavier substituents seem unlikely to exert significant influences on the doorway vibrations which are those strongly coupled to motions of the Fe-CO moiety, but very likely to greatly increase the density of intramolecular states which provide a bath for irreversible decay of excited doorway vibrations.

V. Concluding Remarks

We have made direct measurements of molecular energy transfer at the active site of a protein using intense tunable mid-IR pulses from an FEL to measure the loss of vibrational energy from CO bound to a bare water-soluble heme and CO bound to the active sites of different conformational substates of a heme protein. We have determined that different conformational substates of the same protein, Mb, have different energy transfer rates at the active sites. By examining data obtained on a variety of systems containing protoheme (Ph), we have found that increasing the CO stretching frequency decreases the VR rate, which indicates that VR of excited CO becomes more efficient as external influences cause the CO stretching frequency to be lowered from the ~1970 cm^{-1} value observed in compounds where CO lies nearly perpendicular to the heme plane. This observation suggests the intriguing possibility of controlling or tuning the vibrational relaxation rate by changing the molecular architecture through genetic engineering of the surrounding protein.

The CO vibrational lifetime measurements should be of particular importance in investigating the accuracy of molecular dynamics simulations of heme proteins. Unlike previously studied picosecond time scale processes occurring at the heme, such as ligand rebinding,[35] photodissociation,[37] and vibrational cooling,[38] simulating the VR of the CO ligand does not require assumptions about transitions between different heme electronic states (e.g., refs 31, 37, and 38). The VR of excited CO occurs on the time scale readily accessible to molecular dynamics calculations (0−0.1 ns), and the entire process occurs on the ground electronic potential surface. Because the VR rate is sensitive to protein conformation, molecular dynamics studies of VR at the active site of different heme proteins, providing a range of heme pocket structures, could be an important method to understand the detailed relationships between protein structure and dynamical behavior.

Acknowledgment. We thank Prof. Alan Schwettman and Prof. Todd Smith and their research groups for making it possible to perform the experiments at the Stanford Free Electron Laser Center. Support was provided by the Medical Free Electron Laser program through the Office of Naval Research by Grant N00014-91-C-0170. M.D.F., A.T., B.S., and D.Z. acknowledge additional support from National Science Foundation Grant DMR-90-22675. B.S. thanks the Alexander von Humboldt Foundation for a Feodor Lynen Fellowship. D.D.D.

and J.R.H. acknowledge additional support from National Science Foundation Grant DMR-91-04130. We thank Prof. Kenneth Suslick and Mr. Michael Rosenblatt, who synthesized Fe:TPPS.

References and Notes

(1) Antonini, E.; Brunori, M. *Hemoglobin and Myoglobin in Their Reactions with Ligands*; North Holland: Amsterdam, 1971.

(2) Alben, J. O.; Caughy, W. S. *Biochem.* **1968**, *7*, 175. Caughey, W. S.; Shimada, H.; Choc, M. C.; Tucker, M. P. *Proc. Natl. Acad. Sci. U.S.A.* **1981**, *78*, 2903.

(3) (a) Alben, J. O.; Beece, D.; Bowne, S. F.; Doster, W.; Eisenstein, L.; Frauenfelder; Good, D.; McDonald, J. D.; Marden, M. C.; Moh, P. P.; Reinisch, L.; Reynolds, A. H.; Shyamsunder, E.; Yue, K. T. *Proc. Natl. Acad. Sci. U.S.A.* **1982**, *79*, 3744. (b) Ormos, P.; Braunstein, D.; Frauenfelder, H.; Hong, M. K.; Lin, S.-L.; Sauke, T. B.; Young, R. D. *Proc. Natl. Acad. Sci. U.S.A.* **1988**, *85*, 8492.

(4) Ansari, A.; Berendzen, J.; Braunstein, D.; Cowen, B. R.; Frauenfelder, H.; Hong, M. K.; Iben, I. E. T.; Johnson, J. B.; Ormos, P.; Sauke, T. B.; Scholl, R.; Schulte, A.; Steinbach, P. J.; Vittitow, J.; Young, R. D. *Biophys. Chem.* **1987**, *26*, 337.

(5) Iben, I. E. T.; Braunstein, D.; Doster, W.; Frauenfelder, H.; Hong, M. K.; Johnson, J. B.; Luck, S.; Ormos, P.; Schulte, A.; Steinbach, P. J.; Xie, A. H.; Young, R. D. *Phys. Rev. Lett.* **1989**, *62*, 1916.

(6) Moore, J. N.; Hansen, P. A.; Hochstrasser, R. M. *Chem. Phys. Lett.* **1987**, *138*, 110. Locke, B.; Diller, R.; Hochstrasser, R. M. In *Biomolecular Spectroscopy Part B*; Clarke, R. J. H., Hester, R. E., Eds.; Wiley: Chichester, U.K., 1993; p 1.

(7) Rothberg, L.; Jedju, T. M.; Austin, R. H. *Biophys. J.* **1990**, *57*, 369.

(8) Hong, M. K.; Shyamsunder, E.; Austin, R. H.; Gerstman, B. S.; Chan, S. S. *Phys. Rev. Lett.* **1991**, *66*, 2673.

(9) Owrutsky, J. C.; Li, M.; Culver, J. P.; Sarisky, M. J.; Yodh, A. G.; Hochstrasser, R. M. (*Time-Resolved Vibrational Spectroscopy VI*; Springer Proc. Phys. Springer: New York, 1993.

(10) Hochstrasser, R. M. *Proc. SPIE-Int. Soc. Opt. Eng.* **1993**, 1921 (Laser Spectroscopy of Biomolecules) 16.

(11) Hill, J. R.; Chen, S.; Dlott, D. D.; Tokmakoff, A.; Sauter, B.; Zindars, D.; Fayer, M. D. *Proc. SPIE*, in press.

(12) Heilweil, E. J.; Cavanagh, R. R.; Stephenson, J. C. *Chem. Phys. Lett.* **1987**, *134*, 181. Heilweil, E. J.; Cavanagh, R. R.; Stephenson, J. C. *J. Chem. Phys.* **1988**, *89*, 230. Heilweil, E. J.; Cavanagh, R. R.; Stephenson, J. C. *J. Chem. Phys.* **1988**, *89*, 5342. Heilweil, E. J.; Stephenson, J. C.; Cavanagh, R. R. *J. Phys. Chem.* **1988**, *92*, 6099.

(13) Tokmakoff, A.; Sauter, B.; Fayer, M. D. *J. Chem. Phys.* **1994**, *100*, 9035.

(14) Zimdars, D.; Tokmakoff, A.; Chen, S.; Greenfield, S. R.; Fayer, M. D.; Smith, T. I. Schwettman, H. A. *Phys. Rev. Lett.* **1993**, *70*, 2718. Tokmakoff, A.; Zimdars, D.; Sauter, B.; Francis, R. S.; Kwok, A. S.; Fayer, M. D. *J. Chem. Phys.* **1994**, *101*, 1741.

(15) Young, R. D.; Frauenfelder, H.; Johnson, J. B.; Lamb, D. C.; Nienhaus, G. U.; Philipp, R.; Scholl, R. *Chem. Phys.* **1991**, *158*, 315.

(16) Oldfield, E., Guo, K.; Augspurger, J. D.; Dykstra, C. E. *J. Am. Chem. Soc.* **1991**, *113*, 7537.

(17) Ray, G. B.; Li, X.-Y.; Ibers, J. A.; Sessler, J. L.; Spiro, T. G. *J. Am. Chem. Soc.* **1994**, *116*, 162.

(18) Dlott, D. D.; Fayer, M. D. *IEEE J. Quantum Electron.* **1991**, *27*, 2697.

(19) Greenfield, S. R.; Bai, Y. S.; Fayer, M. D. *Chem. Phys. Lett.* **1990**, *170*, 133.

(20) Tokmakoff, A.; Marshall, C. D.; Fayer, M. D. *J. Opt. Soc. Am. B.* **1993**, *10*, 1785.

(21) Dlott, D. D. in *Laser Spectroscopy of Solids II*; Yen, W., Eds.; Springer Verlag: Berlin, 1988; p 167.

(22) Klauder, J. R.; Anderson, P. W. *Phys. Rev.* **1962**, *125*, 912. Hu, P.; Hartmann, S. R. *Phys. Rev. B* **1974**, *9*, 1. Mims, W. B. *Phys. Rev.* **1968**, *168*, 370.

(23) Levy, D. *Annu. Rev. Phys. Chem.* **1980**, *31*, 197.

(24) Heller, D. F.; Mukamel, S. *J. Chem. Phys.* **1979**, *70*, 563. Mukamel, S.; Smalley, R. E. *J. Chem. Phys.* **1980**, *73*, 4156.

(25) For an in-depth review, see: *Photoselective Chemistry*; Jortner, J., Levine, R. D., Rice, S. A., Eds.; *Adv. Chem. Phys. v. XLVII*; Wiley: New York, 1981.

(26) Califano, S.; Schettino, V.; Neto, N. *Lattice Dynamics of Molecular Crystals*; Springer-Verlag: Berlin, 1981.

(27) Kitagawa, T.; Ogura, T. In *Biomolecular Spectroscopy Part B*; Clarke, R. J. H., Hester, R. E., Eds.; Wiley: Chichester, U.K., 1993; p 139.

(28) Petrich, J. W.; Martin, J. L. In *Time Resolved Spectroscopy*; Clarke, R. J. H., Hester R. E., Eds.; Wiley: Chichester, U.K., 1989; p 335.

(29) Seeley, G.; Keyes, T. *J. Chem. Phys.* **1989**, *91*, 5581. Xu, B.-C.; Stratt, R. M. *J. Chem. Phys.* **1990**, *92*, 1923. Wu, T. M.; Loring, R. F. *J. Chem. Phys.* **1992**, *97*, 8568.

(30) Brooks, C. L.; Karplus, M.; Pettitt, B. M. *Proteins: A Theoretical Perspective of Dynamics, Structure and Thermodynamics*; Adv. Phys. Chem. Vol. LXXI; Wiley: New York, 1988.

(31) Li, H.; Elber, R.; Straub, J. E., *J. Biol. Chem.* **1993**, *268*, 17908.

(32) Austin, R. H.; Beeson, K. W.; Eisenstein, L.; Frauenfelder, H.; Gunsalus, I. C. *Biochemistry* **1975**, *14*, 5355. Elber, R.; Karplus, M. *Science* **1987**, *235*, 318.

(33) Agmon, N.; Hopfield, J. J. *J. Chem. Phys.* **1983**, *79*, 2042. Srajer, V.; Reinisch, L.; Champion, P. M. *J. Am. Chem. Soc.* **1988**, *110*, 6656. Lambright, D. G.; Balasubrumanian, S.; Boxer, S. G. *Biochemistry* **1993**, *32*, 10116.

(34) Powers, L.; Chance, B.; Chance, M.; Campbell, B.; Friedman, J.; Khalid, S.; Kumar, C.; Naqui, A.; Reddy, K. S.; Zhou, Y. *Biochemistry* **1987**, *26*, 4785. Elber, R.; Karplus, M. *J. Am. Chem. Soc.* **1990**, *112*, 9161. Chatfield, M. D.; Walda, K. N.; Magde, D. *J. Am. Chem. Soc.* **1990**, *112*, 4680.

(35) Case, D. A.; Karplus, M. *Mol. Biol.* **1979**, *132*, 343.

(36) Springer, B. A.; Sligar, S. G. *Proc. Natl. Acad. Sci. U.S.A.* **1987**, *84*, 8961. Balasubramanian, S.; Lambright, D. G.; Boxer, S. G. *Proc. Natl. Acad. Sci. U.S.A.* **1993**, *90*, 4718. Braunstein, D. P.; Chu, K.; Egeberg, K. D.; Frauenfelder, H.; Mourant, J. R.; Nienhaus, G. U.; Ormos, P.; Sligar, S. G.; Springer, B. A.; Young, R. D. *Biophys. J.* **1993**, *65*, 2447.

(37) Henry, E. R.; Levitt M.; Eaton, W. A. *Proc. Natl. Acad. Sci. U.S.A.* **1985**, *82*, 2034. Sassaroli M.; Rousseau, D. L.; *J. Biol. Chem.* **1986**, *261*, 16292.

(38) Henry, E. R.; Eaton, W. A.; Hochstrasser, R. M. *Proc. Natl. Acad. Sci. U.S.A.* **1986**, *83*, 8982.